ASSESSING HYDROTHERMAL ALTERATION EFFECTS ON BULK-ROCK GEOCHEMISRY: A CASE EXAMPLE OF WELL OW-910 AT OLKARIA GEOTHERMAL FIELD, KENYA

Victor Otieno
Kenya Electricity Generating Company Ltd.
P.O Box 785-20117 Naivasha
KENYA
votieno@kengen.co.ke; kotienovic@gmail.com

Key words: Olkaria geothermal field, petrochemistry, lithological units, major and trace elements, hydrothermal alteration, element mobility

ABSTRACT

An important step in studying volcanic processes is to understand the sequences along which the magmas evolve. Chemical variations within a group of major and trace elements are usually the result of magma evolution processes. The majority of the trends observed for these two groups of elements against the differentiation index clearly demonstrate that the magma modification process is dominated by crystal-liquid segregation. Studies of the chemical changes imposed on the volcanic rocks from the study well has been vital in quantifying element mobility. The latter has proved to be an important tool in getting a better understanding of the hydrothermal alteration processes affecting the volcanic rocks from well OW-910. The concept of scattering of elemental concentration has proved that some mobilisation has occurred and this principle can successfully be applied, though to a limited extent, to equally assess the effects of hydrothermal alteration on both major and trace element geochemistry. It has been satisfactorily established that mobile elements display some leaching by hydrothermal fluids, even though the degree varies. Immobile elements, on the other hand have remained relatively inert, thus do not appear to be affected by fluid components of alteration processes.

1. INTRODUCTION

The geothermal field in Olkaria is a consequence of the Olkaria Volcanic Complex (OVC). The latter is a young (~ 20 ka), salic volcanic complex located within the central sector of the Kenya Rift Valley (KRV) (Figure 1). It forms part of the Central Kenya peralkaline province (CKPP), a unique assemblage of peralkaline silicic magmatic systems (Macdonald and Scaillet, 2006). The location of the CKPP coincides with the apical region of the Kenya dome, an area of crustal upwarping associated with minor (~ 1 km) amounts of uplift. Eruption of basaltic and trachytic magmas are also evident on the periphery of the OVC. Extensive development of geothermal resources has taken place in Olkaria since the 1980s. The geothermal field has been divided into seven sub-fields for ease of development and management. These include, Olkaria East, Central, Northeast, Southeast, Southwest, Northwest and Domes fields. Presently, the geothermal field has an aggregate installed capacity of ~ 654 MWe. Studies of volcanic systems provide powerful insights to our understanding of how such systems are initiated and evolve over time. Petrogenetic mechanisms normally constitute the main evolutionary phase of transforming the volcanic eruptive products (Macdonald et al., 2014).

1.1 Objectives

The primary objective of this paper is to place constraints on the major magmatic differentiation mechanism responsible for the generation of the rocks of the study well. Of related interest also is

evaluating the scale of hydrothermal alteration on the chemical elements of the altered rocks. Expectedly, detailed interpretation of major and trace element data will provide a deep understanding in achieving the study objectives.

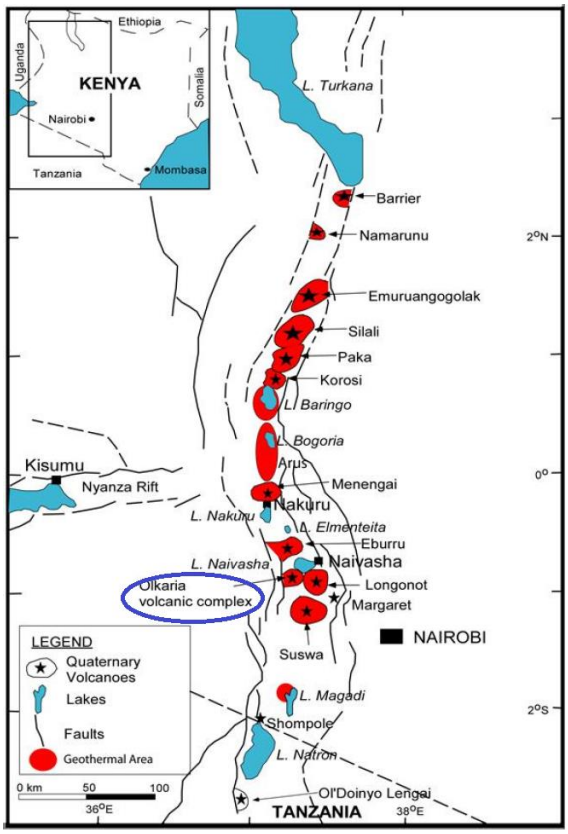

Figure 1: Map of the KRS showing the location of Olkaria Volcanic Complex and other surrounding volcanic centres (Ofwona et al., 2006).

1.2. Overview of well OW-910

Well OW-910 is a vertical well drilled between December 2009 and February 2010 at surface coordinates X= 203732; Y= 9899738 and Z= 1995 masl. It is a production well located in the Domes sub-field, and has a production capacity of about 8 MWe. Presently, the well is connected to Olkaria IV power plant. The lithological units intersected by the well, deduced through binocular, petrographic and ICP-OES analysis are presented in Figure 2. Some of the high temperature alteration minerals encountered in this well encompass epidote, prehnite, wollastonite, actinolite and garnet.

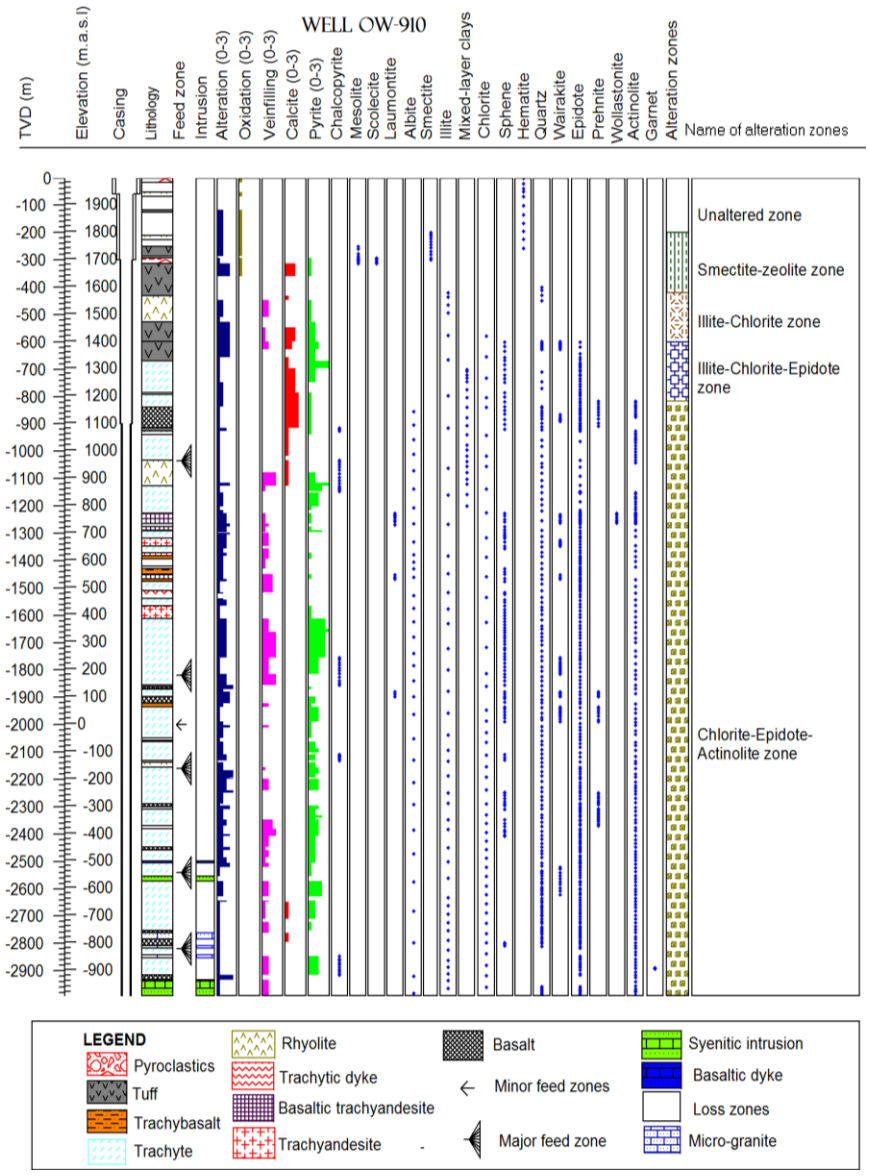

Figure 2: Lithostratigraphic units, alteration minerals and alteration zones of well OW-910

2. GEOLOGICAL BACKGROUND

Olkaria is a Quaternary central volcanic complex in the central sector of the KRV. The geology of the area has been extensively described by, *inter alios*, Clarke et al. (1990), Omenda (1998), etc. Briefly, the surface geology is dominated by comenditic lavas, pumice fall and pyroclastics (Figure 3). On the other hand, the sub-surface geology, as revealed by data from geothermal wells is comprised of (from the youngest to the oldest) Upper Olkaria volcanics, Olkaria basalt, Plateau trachytes and Mau tuffs. The Upper Olkaria volcanics consists mainly of pyroclastics and comendites with occassional interbeds of basalt and trachyte. This unit has been dated at < 0.95 Ma (Omenda, 1998). Its thickness varies between 80 and 350 m.

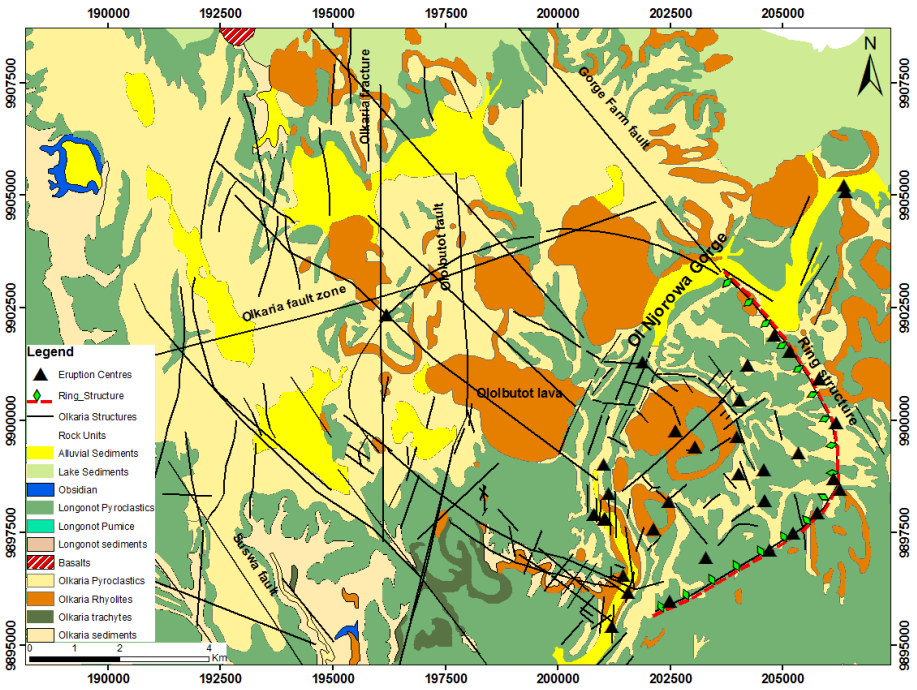

Figure 3: Geological map of the Olkaria Volcanic Complex and the surrounding area (modified from Clarke et al., 1990).

The Olkaria basalt, dated at < 1.65 Ma is dominated by basaltic lavas, interspersed with thin horizons of tuffs, trachytes and rhyolites. The unit has been intersected by most wells at between 400 and 800 m depth. Also, the unit forms the cap-rock and has been used as an excellent marker horizon within the geothermal east field. The Olkaria basalt is preceded by Plateau trachytes which are of Pleistocene age. The unit is dominated by trachyte as the principal rock type, although thin horizons of tuffs, rhyolites and basalts have also been encountered. Trachyte is the reservoir rock for Olkaria East, Northeast, Southeast and Domes sub-fields. Based on the wells' data from these sub-fields, the thickness of this unit has been estimated to be > 1.5 km. The Mau tuffs are the oldest rocks (dated between 3.4-4.5 Ma) encountered within the complex and are of uncertain thickness. The formation has been intersected only by the wells in the Olkaria west fields (Northwest and Southwest), where it forms the reservoir rock.

3. SAMPLING AND ANALYTICAL DETAILS

For this study, forty two samples were systematically analysed to represent the range of rock types in the study well using the Spectro Ciros 500 ICP-OES equipment at the University of Iceland. In all cases, homogeneous but representative samples, devoid of contamination by foreign fragments were selected for analysis. However, in certain cases where minor contamination was evident, all the foreign fragments were carefully removed by the use of a tweezer. For description of the samples, refer to Musonye (2015). The samples were ground in agate mortar to a fineness of approximately 100 mesh powder and weighed in an epicure graphite crucible. This was preceded by melting of the samples in an electric furnace, heated at 1000 ^{o}C for at least 30 mins (after preparing the external reproducibility and internal calibration working standards) and thereafter left to cool for another 15-20 mins. Each fused bead was then transferred into a bottle containing 30 ml of Rockan complexing acid before generating the final results. The major element oxides analysed are SiO_2, Al_2O_3, FeO, MnO, MgO, CaO, Na_2O, K_2O, TiO_2 and P_2O_5. Trace elements analysed include, Ba, Co, Cr, Cu, La, Ni, Rb, Sc, Sr, V, Y, Zn and Zr.

Samples were analysed using the following USGS internationally recognized standards and error margins; (1) Basalts: multiple measurements of standard Basalt, Hawaiian Volcano Observatory (BHVO)-1 2σ (external reproducibility). Analysis for Si, Al, Fe, Mn, Mg, Ca, Na and P was done with 2σ <1.8%. The error margin for trace elements in basalts ranged between 4-8%, (2) Rhyolites: measurements of standard Rhyolite, Glass Mountain (RGM)-1. Elements were analysed with 2σ values as follows; Si and Mg ~ 1%, Ti <2%, Al, Ca, Fe, Na and K <4-6%, Mn and P <8%. The error margin for trace elements in rhyolites is the same as for basalt.

4. RESULTS

4.1 Classification of rock types

To assess the range of compositions, samples from the study well were plotted on the total alkali ($Na_2O + K_2O$) versus. silica (SiO_2) (TAS) as shown in Figure 4. The concentrations of the major elements have been re-calculated to 100% on a volatile free basis and are plotted as such on the TAS diagram.

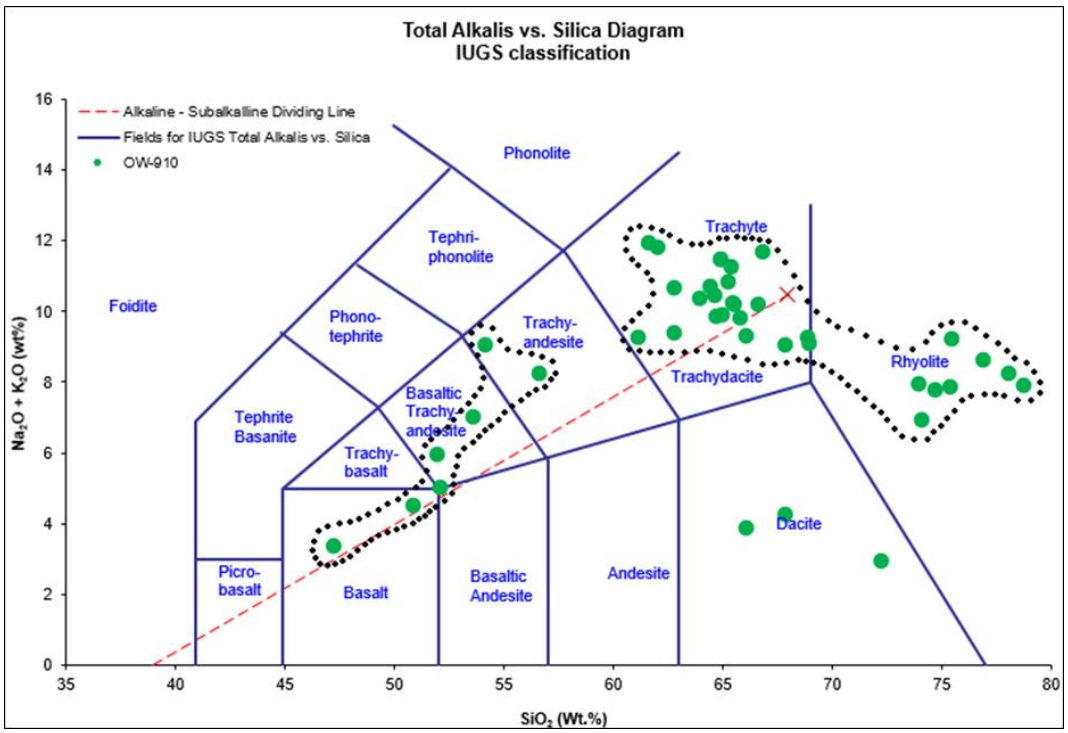

Figure 4: TAS diagram showing the compositional range for sub-surface rocks from well OW-910, according to Le Bas et al. (1986).

From Figure 4, it is evident that the alkaline rocks range from basalt through basaltic trachyandesite, trachyandesite to trachyte. In contrast, the sub-alkaline rocks vary from dacite, trachydacite to rhyolite. The prevalence (~ 90%) of evolved rocks is however, noticeable, depicting a wide range of SiO_2 (61-78 wt. %) (Table 1). A large volume of the salic differentiates cluster to a greater extent in the trachyte and rhyolite fields.

4.2 Major element geochemistry

Variation diagrams of selected major element as a function of SiO_2, as the abscissa are presented in Figure 5. SiO_2 has been chosen as the index of differentiation owing to its abundance and wide concentration range (47-78 wt. %). Generally, rocks in well OW-910 display significant variations in major element concentrations. Mafic and intermediate rock suites show a homogeneous trend for FeO,

MgO and CaO, all showing a negative correlation with increase in SiO_2 contents. The elements are enriched but show a restricted range in the mafic and intermediate rocks at between 9-14 wt.%, 1-7 wt.% and 3-11 wt.%, respectively. In contrast, they are relatively depleted in the highly evolved rocks. For example, FeO depict low abundance (4-8 wt.%) in the evolved rocks, whereas, the contents of MgO and CaO ranges between 0.03-0.43 wt. % and 0.21-2.65 wt. %, respectively in the same rocks.

Similarly, TiO_2 exhibit a limited range in the mafic and intermediate rocks (1.67-3.43 wt.%) and show a significant decline in the silicic rocks (0.09-1.2 wt.%). The decline is more pronounced in samples with SiO_2 contents ranging between 74-78 wt. %. Al_2O_3 contents in all the samples range between 10.31-16.75 wt.% (Table 1). It depicts a narrow range in the mafic and intermediate rocks (13.48-15.73 wt.%) as compared to the highly silicic rocks (10.31-16.75 wt.%). The element displays moderate decline with increase in SiO_2 contents for most of the samples. Na_2O and K_2O exhibit an initial positive correlation with increase in SiO_2 contents, and attains a peak at about 65 wt.% for both elements (Figure 5). Beyond 65 wt.%, Na_2O shows a decrease, whereas, K_2O appears to assume a flat trend with further increase in SiO_2 content.

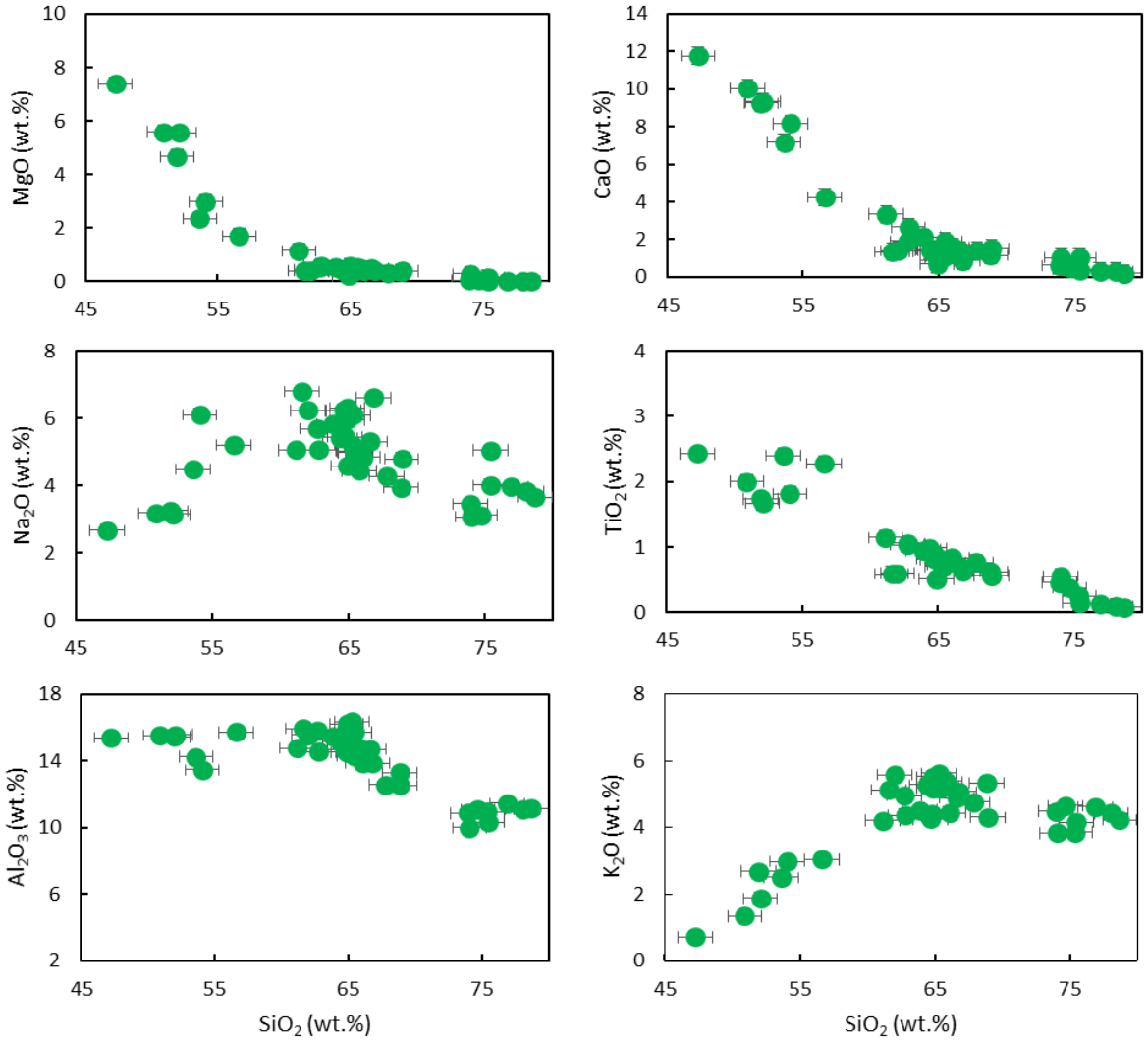

Figure 5: Harker diagrams showing variations of selected major element against SiO_2 for samples from well OW-910.

4.3 Trace element geochemistry

Variations of selected trace elements with SiO_2 are shown in Figure 6. Although the trace element graphics are generally scattered compared to major elements, systematic variations with SiO_2 are still evident. Among the trace elements, the key features observed as differentiation progresses from the mafic to the highly evolved rocks are: (1) ferromagnesian-bearing trace element (which are also the compatible trace elements) such as V, Sr, Ni and Sc exhibit negative correlation with increase in SiO_2 contents, (2) Incompatible trace elements (ITEs) such as Rb and Zr generally show positive correlation with SiO_2. The same case is similar for other ITEs (e.g. La, Y, Ba) not shown in these plots. For instance, V contents decrease from ~ 309 ppm to 120 ppm from the mafic to intermediate rocks (Table 1). The element's content exhibit an abrupt drop down to 4.5 ppm in the highly evolved rocks. The same case is true for Sc, whose contents range between 37-17 ppm in the mafic and intermediate rocks but shows a steep drop (below 7 ppm) and in some cases below the detection limit in a majority of the evolved derivatives. In contrast, ITE such as Zr shows significant increase (> 555 ppm) with increasing SiO_2 contents but is depleted in the mafic and intermediate rocks (438-101 ppm).

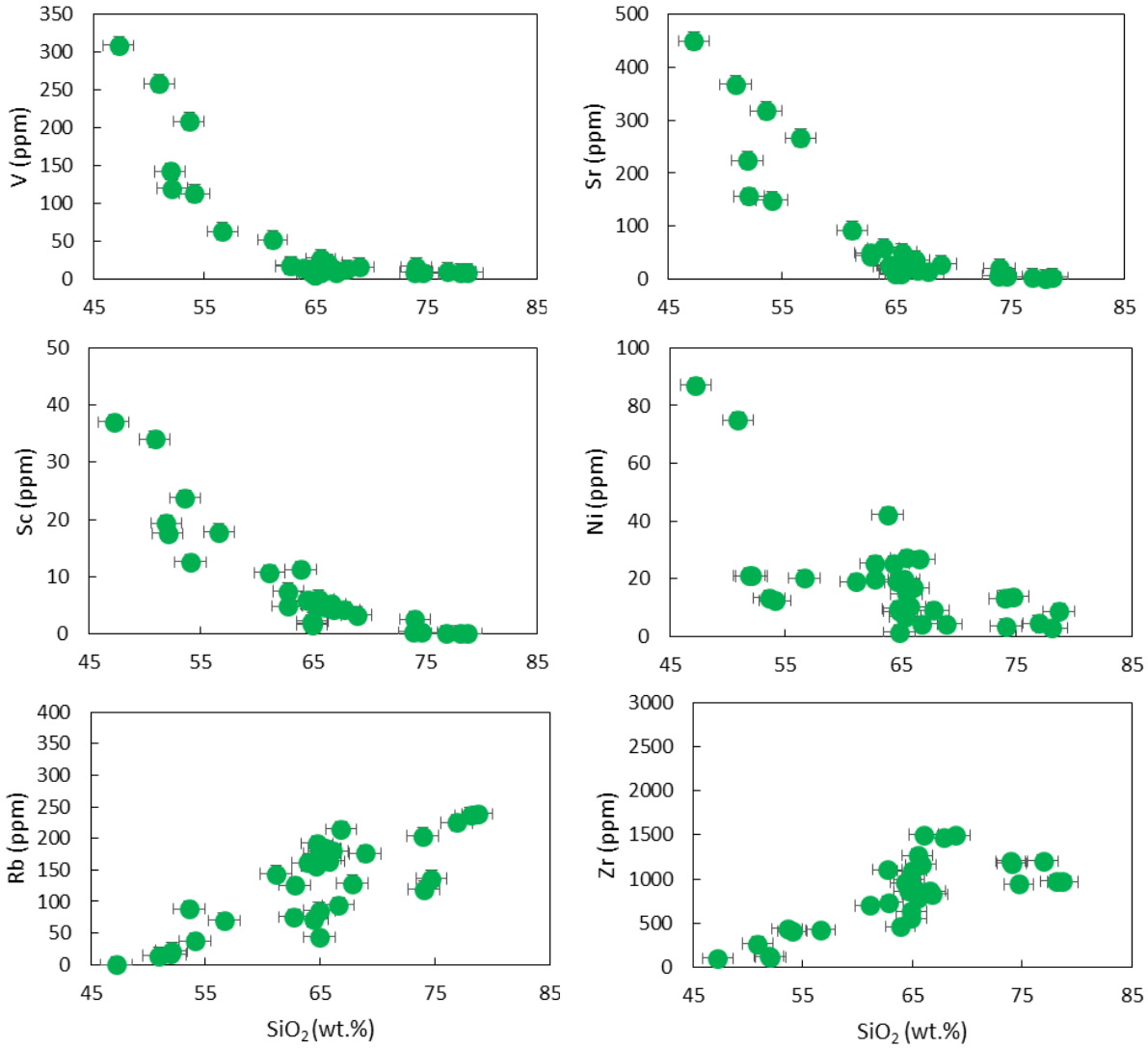

Figure 6: Harker variation diagrams for selected trace elements plotted against the index of differentiation, SiO_2 for samples from well OW-910.

Table 1: Whole rock major and trace element results for well OW-910 based on ICP-OES analysis

WELL OW-910																					
Depth (m)	66	418	436	476	590	722	772	844	894	988	1008	1082	1106	1248	1376	1388	1426	1440	1458	1470	1490
Major elements in wt %																					
SiO_2	75.46	78.70	78.08	76.91	67.84	64.91	64.90	50.92	47.26	62.02	61.59	73.96	74.70	51.93	61.13	56.62	62.79	63.90	53.61	52.09	64.74
Al_2O_3	10.31	11.13	11.08	11.44	13.60	16.21	15.93	15.52	15.40	15.57	15.94	10.85	11.09	15.45	14.78	15.73	14.55	15.48	14.25	15.58	14.65
FeO	3.90	1.78	2.01	2.34	10.20	5.61	5.69	10.72	11.80	7.58	7.60	5.71	5.23	10.40	8.60	9.72	8.21	5.98	12.30	10.17	7.40
MnO	0.06	0.03	0.04	0.05	0.30	0.21	0.18	0.20	0.21	0.27	0.28	0.18	0.13	0.17	0.27	0.17	0.43	0.20	0.32	0.19	0.27
MgO	0.00	0.01	0.00	0.00	0.90	0.23	0.22	5.59	7.38	0.42	0.40	0.05	0.07	4.66	1.15	1.71	0.60	0.53	2.35	5.56	0.45
CaO	0.38	0.21	0.28	0.31	1.32	0.68	0.91	10.03	11.76	1.40	1.34	0.63	0.46	9.26	3.35	4.24	2.65	2.12	7.18	9.33	1.43
Na_2O	5.06	3.66	3.83	3.99	0.18	5.96	6.31	3.19	2.67	6.24	6.81	3.46	3.13	3.26	5.06	5.21	5.06	5.83	4.49	3.15	5.46
K_2O	4.16	4.23	4.42	4.62	4.06	5.53	5.18	1.33	0.70	5.58	5.13	4.49	4.65	2.68	4.21	3.03	4.35	4.52	2.50	1.87	4.42
TiO_2	0.15	0.09	0.10	0.14	1.17	0.52	0.51	2.00	2.43	0.60	0.59	0.46	0.38	1.74	1.15	2.28	1.06	0.96	2.40	1.67	0.89
P_2O_5	0.00	0.00	0.00	0.00	0.15	0.04	0.04	0.33	0.23	0.05	0.05	0.01	0.01	0.25	0.13	1.03	0.15	0.24	0.39	0.27	0.12
Trace elements (ppm)																					
Ba	5.37	4.94	3.72	4.24	153.98	39.61	37.81	302.62	246.57	23.78	21.94	8.07	11.31	1322.29	216.43	1445.01	151.19	1432.03	656.55	491.81	140.34
Co	0.00	0.00	0.00	0.00	16.50	2.55	2.63	47.03	64.22	5.11	4.62	2.63	1.50	42.58	13.25	25.86	14.17	8.71	53.42	45.20	7.51
Cr	2.66	5.12	2.46	4.01	3.35	3.34	3.12	115.94	61.30	5.49	7.33	28.82	6.48	19.60	22.34	12.96	17.48	16.96	24.31	19.63	10.36
Cu	22.91	16.07	16.72	16.84	19.16	12.51	20.73	68.67	94.58	26.89	25.21	16.05	21.30	22.42	26.92	25.11	29.85	34.61	33.67	24.58	15.80
La	187.88	79.56	77.99	82.45	228.91	99.65	112.51	45.71	23.98	300.41	284.87	197.73	161.23	23.19	130.68	79.11	126.07	70.14	88.90	21.75	158.24
Ni	7.52	8.60	2.86	4.55	6.36	1.31	8.59	75.04	87.15	7.10	6.59	13.08	13.80	20.96	18.96	20.21	25.20	42.14	13.27	20.89	9.55
Rb	1690.16	239.22	237.02	225.06	366.31	85.84	176.35	14.36	0.00	91.57	144.33	203.96	136.53	16.71	143.79	70.47	126.05	161.16	88.52	22.04	192.07
Sc	0.10	0.00	0.00	0.00	7.97	1.60	1.88	34.03	37.04	2.33	2.18	0.30	0.24	19.38	10.68	17.79	7.43	11.27	23.79	17.58	5.60
Sr	7.88	3.39	1.88	3.33	31.65	9.24	10.96	368.42	450.03	16.41	12.06	6.13	4.76	224.30	91.99	266.49	44.05	59.61	317.97	156.36	26.42
V	20.76	8.79	9.04	9.66	70.30	4.50	5.15	258.57	309.60	17.32	15.04	9.05	7.62	142.53	51.85	63.14	18.11	14.02	208.44	120.35	12.53
Y	416.15	130.16	131.79	159.50	178.15	67.01	74.60	41.66	21.96	185.47	208.37	145.87	114.70	18.41	90.32	78.11	107.89	59.06	63.43	17.60	109.64
Zn	326.25	139.31	139.15	164.29	265.90	136.61	168.23	130.85	119.21	215.66	233.01	212.64	195.48	74.88	171.29	157.18	167.10	109.67	148.03	88.94	178.74
Zr	2533.54	969.88	977.97	1206.05	1381.12	555.58	634.11	267.54	101.10	1778.28	1814.98	1205.76	941.57	124.81	700.76	424.98	735.04	460.90	438.84	115.53	997.46
Depth (m)	1524	1530	1600	1630	1710	1790	1976	2078	2244	2262	2294	2332	2544	2554	2660	2732	2766	2832	2898	2950	2968
Major elements in wt %																					
SiO_2	72.21	66.03	54.09	67.83	66.06	64.38	68.86	65.47	74.07	64.68	49.65	68.91	64.96	62.74	65.80	65.50	75.40	66.61	65.29	66.83	65.38
Al_2O_3	13.82	16.75	13.48	12.58	13.90	15.15	13.28	14.30	9.98	15.02	13.82	12.55	14.50	15.81	14.76	15.73	10.92	14.69	16.36	13.86	14.50
FeO	7.04	8.89	9.65	7.48	7.36	6.40	5.85	6.24	6.70	6.68	14.33	6.44	7.17	6.70	6.52	5.78	4.01	5.43	4.92	5.26	6.01
MnO	0.14	0.06	0.29	0.26	0.27	0.26	0.23	0.24	0.22	0.27	0.34	0.25	0.39	0.28	0.30	0.26	0.10	0.25	0.25	0.23	0.25
MgO	0.96	1.49	2.98	0.33	0.42	0.43	0.38	0.55	0.28	0.36	3.00	0.40	0.58	0.55	0.47	0.44	0.15	0.48	0.36	0.39	0.43
CaO	1.20	1.30	8.17	1.43	1.57	1.39	1.16	1.89	1.03	1.46	4.50	1.51	1.45	1.91	1.25	1.10	1.04	1.39	1.02	0.87	1.09
Na_2O	0.53	0.29	6.11	4.28	4.85	5.43	3.95	5.02	3.08	6.24	2.58	4.79	4.59	5.69	4.45	4.98	4.01	5.31	5.22	6.62	6.10
K_2O	2.44	3.59	2.97	4.76	4.44	5.28	5.33	5.22	3.83	4.25	6.84	4.30	5.30	4.96	5.39	5.22	3.86	4.89	5.63	5.08	5.17
TiO_2	1.25	1.33	1.82	0.77	0.84	0.99	0.62	0.76	0.56	0.82	3.43	0.57	0.81	1.03	0.77	0.75	0.25	0.70	0.70	0.63	0.81
P_2O_5	0.18	0.16	0.33	0.06	0.06	0.12	0.03	0.08	0.07	0.06	1.29	0.04	0.08	0.12	0.09	0.09	0.02	0.09	0.09	0.08	0.11
Trace elements (ppm)																					
Ba	344.73	219.36	240.90	31.63	40.34	211.08	75.33	154.98	122.85	63.98	458.79	50.99	89.16	199.34	69.28	48.84	22.66	76.23	64.96	40.63	51.61
Co	18.10	20.84	34.58	6.12	6.33	8.23	5.05	8.52	4.24	5.93	56.07	4.21	7.23	9.22	5.25	5.57	2.15	5.02	5.17	4.19	7.66
Cr	34.30	12.29	11.17	20.53	12.10	16.94	9.33	44.70	4.62	14.93	18.62	16.35	3.30	16.34	15.35	20.35	34.62	15.02	15.49	15.20	9.80
Cu	26.37	16.80	23.79	18.00	22.47	27.93	18.40	24.24	12.80	18.31	27.19	16.37	22.04	34.09	22.42	30.86	71.16	26.84	24.18	15.26	15.58
La	150.74	76.86	64.24	232.88	220.07	155.07	256.42	187.20	165.64	174.06	120.02	227.49	179.84	167.93	186.31	147.85	104.97	133.72	142.61	129.72	123.48
Ni	24.58	11.67	12.36	8.91	16.77	25.20	7.95	14.67	3.46	18.96	31.14	4.18	18.85	19.77	10.26	27.16	93.66	26.79	19.90	4.27	6.77
Rb	234.40	33.14	37.56	128.83	179.99	72.70	538.64	167.58	119.48	156.11	54.96	176.11	44.08	75.82	163.81	183.54	234.31	94.63	179.24	214.95	183.60
Sc	10.42	7.04	12.58	4.21	4.65	5.84	3.97	6.16	2.52	5.83	30.23	3.27	2.22	4.85	5.33	5.44	0.85	5.19	5.13	4.22	5.14
Sr	58.76	25.12	149.28	13.15	21.57	24.53	29.07	51.04	20.66	26.13	128.96	28.39	20.89	49.35	26.04	23.19	15.17	36.41	19.21	16.90	10.41
V	102.99	55.70	113.06	13.35	21.58	11.11	25.79	27.39	16.68	9.15	212.09	16.01	13.33	17.19	11.78	8.25	13.21	11.51	9.73	8.44	7.87
Y	123.68	44.23	48.19	150.51	149.31	99.13	153.15	124.12	99.29	100.77	100. 77	120.80	96.60	110.44	113.96	87.37	165.43	90.44	81.33	89.96	92.33
Zn	160.72	154.91	137.91	226.57	189.66	167.71	227.67	198.04	192.90	208.23	251.97	263.05	227.28	184.98	218.22	181.61	223.38	162.77	182.39	116.94	168.53
Zr	914.08	427.46	407.64	1471.50	1503.51	957.13	1578.57	1266.34	1177.86	866.20	596.93	1498.63	1094.34	1105.65	1166.47	779.19	1422.36	862.84	881.65	829.12	834.88

4.4 Hydrothermal alteration effects

Fluid-rock interaction in the geothermal system around well OW-910 has without a doubt changed the contents of the chemical elements in the altered rocks. These fluids deliver the chemical reactants and take away the aqueous reaction products (Pirajno, 1992). To accurately study the potential effects of hydrothermal alteration on mobility of chemical elements, it is vital to compare the chemistry of fresh (unaltered) and altered rocks. However, due to limited data of fresh samples a direct method has been adopted in this study. In using this method, a comparison of elemental concentrations has been applied to assess the effects of hydrothermal alteration on major and trace element geochemistry. This method serves the purpose only to a limited extent. Its major limitation is that it does not put reliable constraints on the effect of alteration on element mobility in altered rocks as compared to other

superior methods (e.g. statistical approach and mass balance calculations), which are known to yield coherent results.

The basic idea of quantification of alteration effects on rock chemistry is based on the concept of element mobility. In this regard, highly mobile elements are characterised by low ionic potential (e.g. Verma et al., 2005) and tend to be easily leached away by the geothermal fluids. These elements exhibits large scatter as a result of the alteration process. On the other hand, highly immobile elements are characterised by high ionic potential and tend to be retained in the host rocks.

4.4.1 Effects on major element geochemistry

A plot of selected major elements (Figure 5) against SiO_2 has equally been applied in this section to interpret alteration effects. SiO_2 has been chosen as the independent variable owing to its ability to remain a nearly conservative element during hydrothermal alteration processes (e.g. Verma et al., 2005). Past studies by the authors' have shown that SiO_2 contents of most geothermal waters are generally low (< 0.15%), hence, the contents in altered rocks are less affected.

4.4.2 Effects on trace element geochemistry

Selected trace elements have been plotted against Zr, as shown in Figure 7 to attempt to decipher the alteration effects on trace element geochemistry. In this case, Zr has been used as a reference variable due to its large range of variation and also being regarded as a highly immobile element in volcanic rocks (e.g. Franzson et al., 2008).

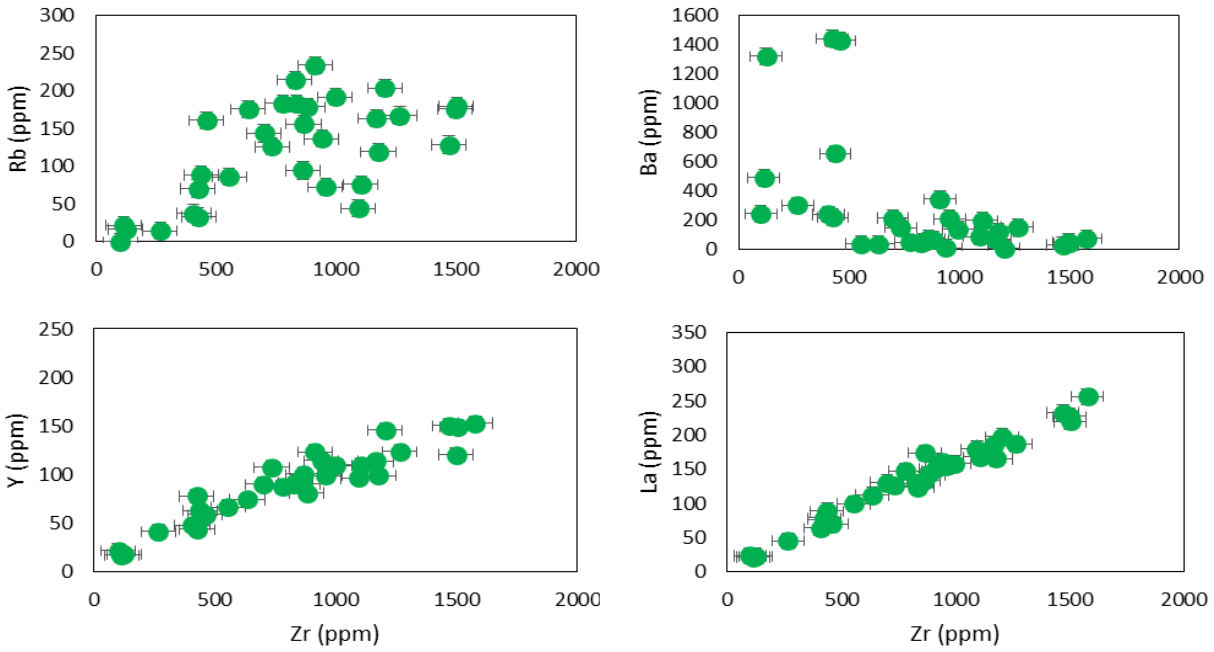

Figure 7: Variation diagrams showing the concentrations of selected trace elements against Zr.

5. DISCUSSION

According to the TAS diagram, (Figure 4), the dominance of evolved rock suites relative to mafic and intermediate rocks signifies high degree of differentiation of the parental magma. Peccerilo et al. (2007) observed that the relative scarcity of the intermediate rocks are related to their high viscosity, which inhibits them from erupting. Even though the more silicic magmas still have high viscosities, they tend to be associated with much lower density. This feature, together with the high volatile contents (e.g. CO_2, H_2O, Cl and F) which commonly characterise these magmas, helps to drive them

out after high degrees of fractional crystallisation from the magma reservoirs (Ronga et al., 2009). Again, based on the TAS classification scheme, the prevalence of trachytes is in accord with the general stratigraphy of Olkaria, which is composed primarily of trachytes (Figure 2) (e.g. Omenda, 1998), except for the Olkaria west fields.

The decrease in Al_2O_3, MgO, CaO and TiO_2 with increasing SiO_2 content (Figure 5) is appropriate with fractional crystallisation of plagioclase and mafic phases, such as clinopyroxene or olivine, which are some of the frequent mineral phases observed during petrographic analysis of rocks from the study well (Musonye, 2015). The observation made is consistent with the trend displayed by ferromagnesian-bearing trace elements, V, Sr, Ni and Sc. It indicates that the process of crystal-liquid segregation in generating evolved compositions from the mafic parents in well OW-910 is involved. The inverse trend exhibited by MgO is consistent with separation of clinopyroxene and olivine from the melt during the early stages of crystallisation. Similarly, the decrease in CaO strongly indicates that the mafic to intermediate magmas evolved by fractionation of an assemblage dominated by plagioclase and clinopyroxene.

The decrease of TiO_2 is probably a result of fractionation of Fe-Ti oxide, e.g. ilmenite from the intermediate to silicic rock suites. This observation is consistent with the gradual decline in Al_2O_3 contents, which would only require fractionation of plagioclase, and to a lesser degree alkali feldspar (Peccerilo et al., 2007). The down-turn in Na_2O abundances in samples containing greater than 65 wt.% SiO_2 (Figure 5) implies the point at which plagioclase fractionation becomes a controlling factor in the compositional evolution of the residual liquid. Nickel is strongly partitioned into olivine, whereas, V is easily incorporated into clinopyroxene in mafic rocks. Sr partitions largely in plagioclase in mafic rocks, while Sc is known to strongly partition into olivine (Ronga et al., 2009). The relatively linear positive correlation exhibited by Rb and Zr vs. SiO_2 can be interpreted to mark their incompatible behavior, where the melt becomes steadily enriched in these elements as fractionation proceeds.

Based on the variation diagram of selected major elements vs. SiO_2 (Figure 5), it is evident, without a doubt that hydrothermal alteration has had inconsequential MgO, CaO, TiO_2, Al_2O_3 in comparison to Na_2O and K_2O. Large degree of scattering is more pronounced in Na_2O indicating that it has been significantly mobilised by the post-magmatic alteration processes. However, the level of leaching is not extensive in K_2O as is the case with Na_2O. These two elements are traditionally known to be highly mobile during hydrothermal alteration processes (e.g. Verma et al., 2005). The excessive loss of these two elements can also be accountable for the marked metaluminous character (expressed by molar proportions $Al_2O_3 > Na_2O + K_2O$) for most of the samples of the study well. For the selected trace elements vs. Zr (Figure 6), it is noted that Y and La are comparatively inert and not affected hydrothermal alteration processes. Previous studies by Verma et al. (2005) have advocated that these two elements are typical fluid-immobile elements. On the other hand, it is evident that hydrothermal alteration has least affected Ba, but has severely mobilised Rb, as exemplified by wide scattering. Rb, an alkali metal is a major constituent of the alkali feldspars and highly mobile, hence easily leached away by the fluid components of the alteration process. Also, it is key to note that Loss on Ignition (LOI), used as a monitor of the degree of alteration (e.g. Franszon et al., 2008) were not measured for the samples of the study well.

6. CONCLUSION

According to the geochemical whole-rock analysis, rocks of the study well show a complete range of composition from mafics to the highly evolved derivatives (i.e. from basalt to trachyte or rhyolite). Major and trace element systematics suggest that fractional crystallisation is the dominant mechanism for the generation of the strongly evolved rock suites of the study well. However, the author refuses to rule out completely other magma modification mechanisms, no matter limited role they played. Significant changes in the abundance of major oxides and trace elements have not taken place during hydrothermal alteration processes. Nevertheless, some elements are observed to have been extensively mobilised by the fluid components of the hydrothermal alteration processes.

7. RECOMMENDATION

Considering that assessment of hydrothermal alteration on bulk rock chemistry in this study was based exclusively on altered rocks, geochemistry data of fresh (unaltered) samples should be taken into account for better interpretation.

ACKNOWLEDGEMENTS

The author would like to thank the University of Iceland, Faculty of Earth Sciences for analysis of the samples. In addition, the author thank Michael Mwania for his constructive criticism and comments and his improvement of the content of this document.

REFERENCES

Clarke, M.C.G., Woodhall, D.G., Allen, D., Darling, G., 1990: Geological, Volcanological and hydrogeological controls of the occurrence of geothermal activity in the area surrounding Lake Naivasha, Kenya. Min. of Energy, Nairobi, report 150, 138 pp.

Franzson, H., Zierenberg, R. and Schiffman, P., 2008: Chemical transport in geothermal systems in Iceland, Evidence from hydrothermal alteration. Journal of Volcanology and Geothermal Research, Volume 173, p. 217-229.

Le Bas, M.J., Le Maitre, R.W., Streckeisen, A., and Zanettin, B., 1986: A chemical classification of volcanic rocks based on the total alkali-silica diagram: Journal of Petrology, v. 27, no. 3, p. 745-750.

Macdonald, R., Baginski, B., and Upton, B. G. J., 2014: The volcano–pluton interface; The Longonot (Kenya) and Kûngnât (Greenland) peralkaline complexes. J. Petrology, p. 232-241.

Macdonald, R., Scaillet, B., 2006: The central Kenya peralkaline province: Insights into the evolution of peralkaline salic magmas. J. Petrology, p. 59-73.

Musonye, X.S., 2015: Sub-surface petrochemistry, stratigraphy and hydrothermal alteration of the Domes area, Olkaria geothermal field, Kenya, University of Iceland, MSc. Thesis, p. 1-109.

Ofwona, C., Omenda, P., Mariita, N., Wambugu, J., Mwawongo, G., and Kubo, B., 2006: Surface geothermal exploration of Korosi and Chepchuk prospects. KenGen internal report, 44 pp.

Omenda, P.A., 1998: The geology and structural controls of the Olkaria geothermal system, Kenya. Geothermics, 27-1, p. 55-74.

Peccerillo, A., Donati, C., Santo, A. P., Orlando, A., Yirgu, G., and Ayalew, D., 2007: Petrogenesis of silicic peralkaline rocks in the Ethiopian rift: Geochemical evidence and volcanological implications. Journal of African Earth Sciences 48, p. 161-173.

Pirajno, F., 1992: Hydrothermal Mineral Deposits. John Wiley and Sons, Sydney, 709 pp.

Ronga, F., Lustrini, M., Marzoli, A., and Melluso, L., 2009: Petrogenesis of a basalt-comendite-pantellerite rock suite: the Boseti Volcanic Complex (Main Ethiopian Rift). Miner Petrol, 98, p. 227-243.

Verma, S.P., Torres-Alvarado, I. S., Satir, M., and Dobson, P. F., 2005: Hydrothermal alteration effects in geochemistry and Sr, Nd, Pb and O isotopes of magmas from the Los Azufres geothermal field (Mexico): A statistical approach, Geochemical journal, Vol. 39, p. 141-163.